International Journal of Social Science Research and Review

http://ijssrr.com
editor@ijssrr.com
Volume 8, Issue 5
May, 2025
Pages: 124-131

Assessment of the Economic Significance of Gold: A Reappraisal of the Ilesha Schist Belt, Southwestern Nigeria

Ahmed K. Usman[1,2]; Mahmood Umar[1]; Bala Balarabe[1]; Yusuf A. Hassan[1]; Aliyu Muhammad[1]; Saidat O. Abdulrasheed[3]

[1] Physics Department, Ahmadu Bello University, Zaria, Nigeria

[2] Faculty of Natural Sciences, Comenius University, Bratislava, Slovakia

[3] Pan African University, PAUWES, Algeria

E-mail: ahmedkehindeusman@gmail.com; akusman@abu.edu.ng

http://dx.doi.org/10.47814/ijssrr.v8i5.2714

Abstract

Nigeria, endowed with significant gold deposits, holds substantial economic potential, particularly in the northwest and southwest regions within the Schist Belts. In the Iperindo axis of the Ilesha Schist Belt, artisanal mining has been reported; however, the lack of comprehensive geoscience data hinders optimal resource development. This study evaluates the economic viability of gold occurrences in the area, leveraging geoscience research findings. To assess gold mineralization potential, Geonics EM34-3 and SuperSting R8/IP/SP meters were used for frequency domain electromagnetic (FDEM) and electrical resistivity tomography (ERT) profiling, alongside geochemical sampling of soil and stream sediments. Apparent resistivity data from ERT profiles were inverted using RES2DINV software, while Oasis Montaj was utilized to generate 2D conductivity/resistivity sections, maps, and 3D subsurface models. The results suggest the presence of gold or base metals in pegmatitic veins within low-resistivity, high-conductivity zones. Additionally, processed geochemical data identified areas with substantial mineralization potential. These findings underscore the economic potential for commercial gold exploitation in the Ilesha Schist Belt. Instead of further expanding artisanal mining, structured commercial development could enable the government to collect royalty taxes, create employment opportunities, and foster economic growth for both the local community and the nation.

Keywords: *Gold Mineralization; Low Resistivity / High Conductivity Zones; Pegmatitic Veins; Threshold; Iperindo*

International Journal of Social Science Research and Review

Volume 8, Issue 5
May, 2025

Introduction

Nigeria, endowed with significant gold deposits, holds substantial economic potential, particularly in the northwest and southwest regions within the Schist Belts. Artisanal mining has been reported in the Iperindo axis of the Ilesha Schist Belt; however, the lack of comprehensive geoscience data hinders optimal resource development. Nigeria's gold mineralization is orogenic, meaning it is controlled by deep-seated fractures. It occurs in amphibolites in the Ilesha and Egbe areas, where concentrations exceed the typical primary gold content for similar rock types (Osinowo *et al.*, 2020). This study reviews the works of Osinowo *et al.* (2020), Usman *et al.* (2020) and Usman *et al.* (2021) to assess the economic viability of gold occurrences in the area. The reviewed studies employed Geonics EM34-3 and SuperSting R8/IP/SP meters for frequency domain electromagnetic (FDEM) and electrical resistivity tomography (ERT) profiling, along with soil and stream sediment geochemical sampling to evaluate gold mineralization potential. Research has shown that ERT provides accurate subsurface conductivity distribution data, which is essential for identifying metal deposits (Osinowo *et al.*, 2020). Electromagnetic (EM) methods, which measure the ease of electric current flow through the earth, rely on the ground's response to a propagating alternating field. An alternating current flows through either a large loop of wire or a small coil with multiple wire turns (Usman *et al.*, 2021). The apparent ground conductivity σ_a (equation 1) is measured by electromagnetic technology and depends on various factors such as coil separation (s), operating frequency f, magnetic permeability of the vacuum, and the ratio of the amplitudes of the primary and secondary electromagnetic fields $\frac{H_s}{H_p}$.

$$\sigma_a = \frac{4}{\omega \mu_0 s^2} \frac{H_s}{H_p} \text{ ……………………(1)}$$

where, $\omega = 2\pi f$. According to Telford *et al*. (1990) and Kearey *et al*. (2002), the depth of investigation depends on the frequency of the inducing field and the conductivity of the propagation medium. Greater penetration occurs at lower frequencies and in terrains with lower conductivity. The reconnaissance study for a pre-geochemical examination aims to identify favorable field features, such as fractures and joints that may serve as mineralization sites, as well as locate streams where sediment samples can be collected.

Study Area

The study area is situated in the Basement Complex of southwest Nigeria, it lies between latitudes 7°25' N and 7°45' N and longitudes 4°35' E and 4°55' E. The area is primarily composed of granite gneiss, with pegmatite veins intruding, along with quartzite and quartz schist that may contain gold (Figure 1). Most of the rocks in the study region mostly strike in a north-south direction and dip in schist between 70° and 80°W and in quartz schist up to 80°W (Usman, 2019).

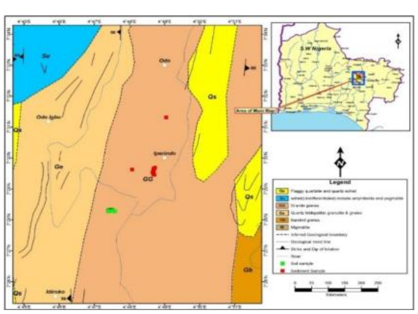

Figure 1a: Geological Map of the Study Area (Adapted from NGSA, 2009)

Figure 1b: Some Rock Outcrops in the Study Area

A multi-electrode SuperSting R8/IP/SP resistivity meter (Figure 2a) was used to collect data for electrical resistivity tomography (ERT). This resistivity meter can simultaneously measure ground resistance at multiple electrode stations along a designated profile, significantly improving efficiency and reducing fieldwork labour (Griffiths *et al.*, 1990). The Geonics EM34-3 Terrain Conductivity Meter was used for electromagnetic (EM) data acquisition (Figure 3a). This frequency domain electromagnetic (FDEM) device interacts with the subsurface, gathering information about the earth's electrical properties using the electromagnetic induction principle. The system consists of transmitter and receiver coils, which are connected via cables to separate console units. The transmitter coil and console generate primary electromagnetic fields, while the receiver coil and console analyze secondary electromagnetic fields and record measurements. As shown in Figures 2b and 3b, five ERT profiles and six EM profiles were established, with a 10 m spacing between profiles, covering a total length of 336 m. For ERT, measurements were conducted using a dipole-dipole electrode configuration with a 3 m dipole spacing (Osinowo *et al.*, 2020; Usman *et al.*, 2021). For geochemical analysis, nine soil samples and eleven stream sediment samples were collected and analyzed at Bureau Veritas Minerals Laboratories, Vancouver, Canada (Usman *et al.*, 2020, Usman *et al.*, 2023).

Figure 2a: Geophysical Crew Deploying ERT meter

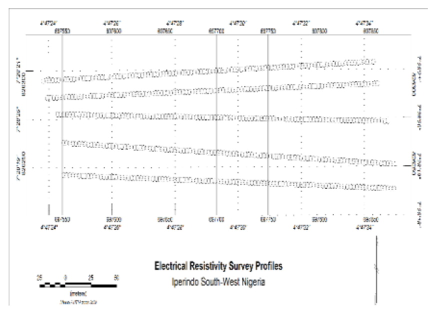

Figure 2b: ERT Survey Profiles Base Map.

Figure 3a: Geophysical Crew Deploying EM Conductivity Meter

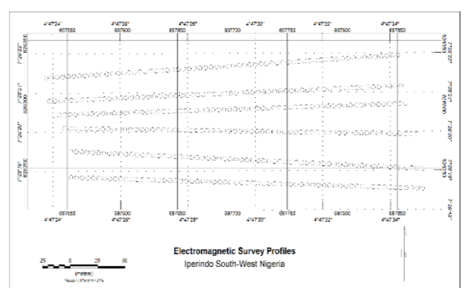

Figure 3b: EM Survey Profiles Base Map.

Data Processing

The resistivity meter directly measured the apparent ground resistivity data, which was then quality-checked (QC) and consistency-verified. Apparent resistivity data from ERT profiles were inverted using Loke and Barker (1996) RES2DINV inversion program, and Oasis Montaj was used to generate 2D conductivity/resistivity sections, maps, and 3D subsurface models (Osinowo *et al.*, 2020; Usman et al., 2021) using kriging gridding techniques (Chiao, 2014). According to Usman *et al.* (2020), the data from the analyzed soil and stream sediment samples were processed with R, SPSS, and MS Excel. These were utilized to assess the ground conductivity distribution's ability to identify anomalous ground conductivity zones, as well as the gold potential of the Iperindo axis inside the Ilesha Schist belt.

Results and Discussions

Table 1 below reveals the ERT profiles that trend along the E-W direction of the study area and are imaged up to 66 m below the surface. The profiles show that the resistivity distribution values range from 3.41 to 18836 **Ω**m for profile 1, 4.41 to 9875 **Ω**m for profile 2, 24.4 to 4572 **Ω**m for profile 3, 6.91 to 134456 **Ω**m for profile 4 and 4.91 to 87000 **Ω**m for profile 5. For all the profiles, three geoelectric layers were delineated. The near-surface overburden layer, about 4 to 9.56 m below the surface, generally displays a relatively low resistivity distribution. The result also presents heterogeneous low-resistivity faults and fractured zones extending up to a depth of about 40 m, that is, having a thickness of about 21.5 to 30.44 m. The final high-resistive fresh basement generally characterizes the deeper part of the subsurface.

Table 1: Summary of Resistivity Layers with Depth and Thickness of the ERT Profiles

Profile No.	No. of Layers	Description	Thickness (m)	Depth (m)	Resistivity Range (Ωm)
1	1	Overburden	5.50	5.50	3.41 – 137
	2	Faults/Fractured Basement	23.5	29.00	4 – 100
	3	Fresh Basement	37.10	66.10	1500 – 18836
2	1	Overburden	7.56	7.56	4.41 – 60
	2	Faults/Fractured Basement	27.94	35.50	14 – 470
	3	Fresh Basement	30.60	66.10	1486 – 9875
3	1	Overburden	5.00	5.00	24.4 – 74.6
	2	Faults/Fractured Basement	13.30	18.30	2.6 – 229
	3	Fresh Basement	47.80	66.10	229 – 4572
4	1	Overburden	4.00	4.00	6.91 – 58.7
	2	Faults/Fractured Basement	21.50	25.50	58.7 – 490
	2	Fresh Basement	40.60	66.10	2818–134456
5	1	Overburden	9.56	9.56	4.91 – 95
	2	Faults/Fractured Basement	30.44	40.00	21.6 – 418
	3	Fresh Basement	26.10	66.10	1802–87000

Table 2 below reveals the EM profiles that trend along the E-W direction of the study area and are imaged up to 60 m below the surface. The profiles show a conductivity distribution that ranges in value from 2.61 to 22.59 mS/m for profile 1, 4.26 to 22.16 mS/m for profile 2, 4.72 to 22.65 mS/m for profile 3, 4.27 to 22.95 mS/m for profile 4, 4.27 to 24.20 mS/m for profile 5, and 4.27 to 22.51 mS/m for profile 6. Three geoelectric layers were delineated for all the profiles. The near-surface overburden layer, about 12.6 to 20.5 m below the surface, generally displays a relatively low conductivity distribution. The result also presents zones with high conductivity distribution values extending up to a depth of about 50 m, that is, having a thickness of about 30.5 to 35.5 m. The final low-conductivity fresh basement generally characterizes the deeper part of the subsurface.

Table 2: Summary of Conductivity Layers with Depth and Thickness of the EM Profiles

Profile No.	No. of Layers	Description	Thickness (m)	Depth (m)	Conductivity Range (mS/m)
1	1	Overburden	14.50	14.50	2.69 – 10.70
	2	Faults/Fractured Basement	30.50	45.00	13.13 – 22.59
	3	Fresh Basement	15.00	60.00	4.61 – 11.76
2	1	Overburden	12.60	12.60	4.26 – 10.98
	2	Faults/Fractured Basement	31.90	44.50	14.83 – 22.16
	3	Fresh Basement	15.50	60.00	5.92 – 14.83
3	1	Overburden	13.00	13.00	4.72 – 11.02
	2	Faults/Fractured Basement	35.50	48.50	12.96 – 22.65
	3	Fresh Basement	11.50	60.00	6.02 – 11.02
4	1	Overburden	15.00	15.00	4.27 – 10.00
	2	Faults/Fractured Basement	34.00	49.00	13.93 – 22.95
	2	Fresh Basement	11.00	60.00	5.90 – 12.09
5	1	Overburden	20.50	20.50	4.27– 12.61
	2	Faults/Fractured Basement	29.5.50	50.00	14.59 – 24.20
	3	Fresh Basement	10.00	60.00	5.92 – 12.61
6	1	Overburden	18.50	18.50	4.27 – 10.43
	2	Faults/Fractured Basement	31.00	49.50	14.09 – 22.51
	3	Fresh Basement	10.50	60.00	6.21 – 12.27

The 3D subsurface conductivity distribution of the research area was delineated using integrated individual georeferenced, filtered, gridded, and depth-sorted conductivity profiles (Figures 4a & b). The figures show that the conductivity values in the entire research region range from less than 4.44 to 22.12 mS/m. The near-surface region is primarily low in apparent conductivity distribution (4.44 to 11.00 mS/m), with isolated high conductivity zones (19.00 to 23.00 mS/m) limited to the study area's eastern and western regions. Additionally, the figures reveal that the bottom section, which corresponds to the fresh or unweathered basement, has low apparent conductivity values.

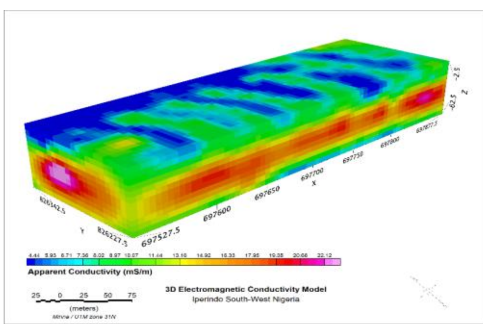

Figure 4a: 3D EM Conductivity Distribution Image of the Study Area

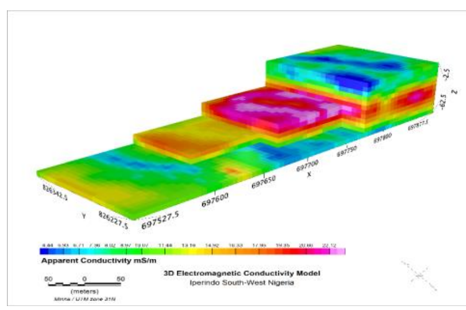

Figure 4b: Sliced EM Conductivity 3D Model to Reveal Desired Parts of the Model.

Elemental Distribution and Relationship

The estimated background values for Au in soil samples and stream sediments for the study area were 1.3 ppb each, and thresholds were 4.44 and 2.60 for soil and stream sediments, respectively. Au concentration ranges from 0.2–5.4 ppb with a mean of 1.36 ppb in soil samples and ranges from 0.4–3.1

ppb with a mean of 1.2 ppb in stream sediments (Tables 3 and 4). As shown in Figure 5a, the stream sediment in location 11 (SS11) has the highest recorded Au content (3.1 ppb), while the stream sediment in location 4 (SS4) has the lowest recorded Au value (0.4 ppb). Soil samples in locations 8 and 9 also have the highest recorded Au content (5.4 ppb) and the lowest recorded Au value (0.2 ppb) (Figure 5b) (Usman *et al.*, 2020).

According to the bivariant plot (Figure 6) that illustrates the correlation between As, Sb, and Au concentrations, Au concentrations are highest in soil samples where As concentrations are relatively high and Sb concentrations are low. This indicates that there is an enrichment (positive correlation) between Au and As (Usman *et al.*, 2020).

Table 3: Metal Distribution Result for Soil Samples

Elements	Soil Samples (n = 9)		Threshold (2SD+Mean)	Calculated Background Values (ppm)
	Range	Mean±SD		
Cu	13.5 – 74.1	42.19±19.18	80.55	42
Pb	46.28 – 68.55	54.97±7.18	69.33	55
Zn	40 – 1197.2	219.06±350.69	920.44	250
Ni	1.8 – 29.7	10.50±7.65	25.80	13
Co	0.9 – 15.4	7.93±5.13	18.19	10
Mn	99 – 568	337.22±185.05	707.32	320
Au (ppb)	0.2 – 5.4	1.36±1.54	4.44	1.3
V	19 – 76	46.67±16.10	78.87	50
Cr	12 – 58	29.56±12.17	53.90	32

Table 4: Metal Distribution Result for Stream Sediments

Elements	Stream Sediments (n=11		Threshold (2SD+Mean)	Calculated Background Values (ppm)
	Range	Mean±SD		
Cu	15.5 – 33.7	26.26±5.93	38.12	28
Pb	39.23 –57.64	47.84±4.95	57.74	48
Zn	189.7 – 1083.5	468.6±245.09	958.78	550
Ni	3.1 – 10.7	5.38±2.55	10.48	8
Co	2.7 – 15	5.48±3.36	12.20	5
Mn	153 – 406	240.55±69.80	380.15	240
Au (ppb)	0.4 – 3.1	1.2±0.70	2.60	1.3
V	17 – 55	26.82±10.00	46.82	28
Cr	12 – 33	17.09±5.84	28.77	18

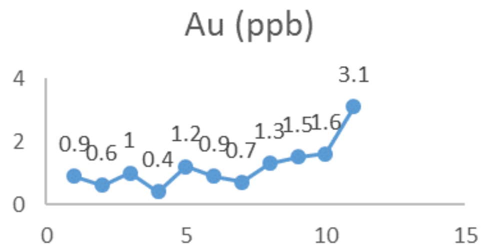

(a)

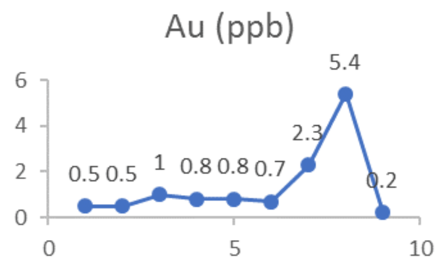

(b)

Figures 5a&b: Au Concentration Distribution

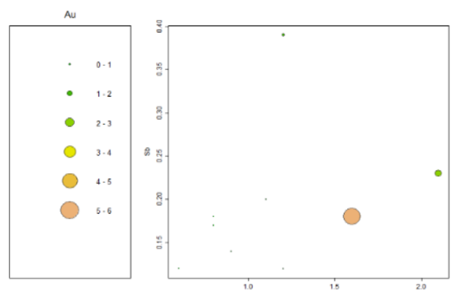

Figure 6: Bivariant Plot Displaying correlation between as, Sb, and Au concentrations

According to Osinowo et al. (2020) and Usman et al. (2021), several discrete zones with high conductivity and low resistivity were identified. These low-resistivity, high-conductivity zones are in the eastern and western parts of the study area and are likely composed of multiple veins and faults saturated with conductive materials such as gold, groundwater, or base metals. These elements are most likely associated with mineralized pegmatitic veins.

Arsenic (As) appears to be the most indicative pathfinder element in the study area, as reported by Usman et al. (2020). The highest concentrations of Au were detected in the analyzed soil and stream sediment samples, exceeding the statistical threshold used to distinguish background levels from gold anomalies. The computed background Au concentration for the study area was 1.3 ppb, while values above 1 ppb are considered anomalous and warrant further exploration.

Conclusion

The results indicate potential gold or base metal mineralization within pegmatitic veins located in low-resistivity and high-conductivity zones. Processed geochemical data further highlight areas with significant mineralization potential. The findings of this study are highly valuable, particularly for the strategic exploitation of gold mineralization in the study area. Rather than merely expanding artisanal mining activities, these insights could support government initiatives in regulating resource extraction, generating revenue through royalty taxes, and fostering job creation and economic growth for both the local community and the nation.

Acknowledgment

The authors express their gratitude to Pan African University for funding this work.

References

Chiao, L., Chen, Y. and Gung, Y. (2014). Constructing empirical resolution diagnostics for kriging and minimum curvature gridding. *J. Geophys. Res.: Solid Earth* 119 (5), 3939-3954. https://doi.org/10.1002/2013JB010364.

Griffiths, D.H., Turnbull, J. and Olayinka, A.I. (1990). Two-Dimensional Resistivity Mapping with a Computer-Controlled Array. *First Break*, 8, 121-129. https://doi.org/10.3997/1365-2397.1990008.

Kearey, P., Brooks, M., & Hill, I. (2002). *An introduction to geophysical exploration* (3rd ed.). Blackwell Science Ltd.

Loke M.H. and Barker, R.D. (1996). Rapid Least-Squares Inversion of Apparent Resistivity Pseudosections by a Quasi-Newton Method. *Geophysical Prospecting*, 44, 131-152. https://doi.org/10.1111/j.1365-2478.1996.tb00142.x.

Nigerian Geological Survey Agency (NGSA). (2009). *Lineament and Geological Map of Nigeria* (Scale 1:100,000).

Osinowo, O.O., Usman, A.K. and Omitoogun, A.A. (2020). Application of Electrical Resistivity Tomography for Mapping Gold Mineralization Potential in Iperindo, Ilesha schist belt, southwestern Nigeria. *International Journal of Advanced Geosciences*, 8(2), 146-152.

Telford, W. M., Geldart, L. P., & Sheriff, R. E. (1990). *Applied geophysics* (2nd ed.). Cambridge University Press.

Usman, A. K. (2019). *Integrated geophysical and geochemical exploration for gold deposit in part of Ilesha Schist Belt, southwestern Nigeria* [Master's thesis, Pan African University Institute of Life and Earth Sciences (PAULESI), University of Ibadan.

Usman, A. K., Osinowo, O. O., Abdulrasheed, S. O. and Usman, Q. T. (2020). Geochemical Characterization of gold and Associated elements in Iperindo, Ilesha Schis Belt, Southwestern Nigeria. P*roceedings of the Nigerian International Materials Congress (NIMACON)*. Vol.1. Pg. 115-118. ISBN 978-060-609-21.

Usman, A. K., Osinowo, O. O., Raimi, J. and Onuh E. (2021). Application of Frequency Domain Electromagnetic for mapping gold mineralization potential in Iperindo, Ilesha schist belt, southwest Nigeria. *Proceedings of the School of Physical Sciences Biennial International Conference (SPSBIC)*. Pg. 180-188.

Usman, A. K., Abdulrasheed, S. O., Hassan, Y. A., Onuh, E. and Aliyu, Y. (2023). A Review of Economic Importance and Viability of Gold: A Case Study of Ilesha Schist Belt, Southwestern Nigeria. *Proceedings of the 13th International Conference on Agriculture, Animal Science and Rural Development*. Pg. 510-520. ISBN: 978-1-955094-66-5.

Copyrights

Copyright for this article is retained by the author(s), with first publication rights granted to the journal.

This is an open-access article distributed under the terms and conditions of the Creative Commons Attribution license (http://creativecommons.org/licenses/by/4.0/).